

# A cross-biome comparison of daily light use efficiency for gross primary production

DAVID P. TURNER\*, SHAWN URBANSKI†, DALE BREMER‡, STEVEN C. WOFSY†, TILDEN MEYERS§, STITH T. GOWER¶ and MATTHEW GREGORY\*

\*Department of Forest Science, Oregon State University, Corvallis, OR 97331-7501, USA, †Earth and Planetary Sciences, Division of Engineering and Applied Sciences, Harvard University, Cambridge, MA 02138, USA, ‡Kansas State University, Department of Horticulture, Forestry and Recreational Resources, Manhattan, KS 66506-4901, USA, §National Oceanic and Atmospheric Administration, Atmospheric Turbulence and Diffusion Division, Oak Ridge, TN 37831-2456, USA, ¶Department of Forest Ecology and Management, University of Wisconsin, Madison, WI 53706, USA

## Abstract

Vegetation light use efficiency is a key physiological parameter at the canopy scale, and at the daily time step is a component of remote sensing algorithms for scaling gross primary production (GPP) and net primary production (NPP) over regional to global domains. For the purposes of calibrating and validating the light use efficiency ( $\epsilon_g$ ) algorithms, the components of  $\epsilon_g$  – absorbed photosynthetically active radiation (APAR) and ecosystem GPP – must be measured in a variety of environments. Micrometeorological and mass flux measurements at eddy covariance flux towers can be used to estimate APAR and GPP, and the emerging network of flux tower sites offers the opportunity to investigate spatial and temporal patterns in  $\epsilon_g$  at the daily time step. In this study, we examined the relationship of daily GPP to APAR, and relationships of  $\epsilon_g$  to climatic variables, at four micrometeorological flux tower sites – an agricultural field, a tallgrass prairie, a deciduous forest, and a boreal forest. The relationship of GPP to APAR was close to linear at the tallgrass prairie site but more nearly hyperbolic at the other sites. The sites differed in the mean and range of daily  $\epsilon_g$ , with higher values associated with the agricultural field than the boreal forest.  $\epsilon_g$  decreased with increasing APAR at all sites, a function of mid-day saturation of GPP and higher  $\epsilon_g$  under overcast conditions.  $\epsilon_g$  was generally not well correlated with vapor pressure deficit or maximum daily temperature. At the agricultural site, a  $\epsilon_g$  decline towards the end of the growing season was associated with a decrease in foliar nitrogen concentration. At the tallgrass prairie site, a decline in  $\epsilon_g$  in August was associated with soil drought. These results support inclusion of parameters for cloudiness and the phenological status of the vegetation, as well as use of biome-specific parameterization, in operational  $\epsilon_g$  algorithms.

*Keywords:* absorbed photosynthetic radiation, carbon cycle, eddy covariance, gross primary production, light use efficiency, remote sensing

*Received 11 December 2001; revised version received 7 May 2002 and accepted 19 July 2002*

## Introduction

Understanding vegetation light use efficiency for gross primary production ( $\epsilon_g$ ) is of interest in relation to application of satellite data for monitoring gross primary production (GPP) and net primary production (NPP) at regional to global scales (Field *et al.*, 1995; Oechel *et al.*,

2000; Running *et al.*, 2000; Behrenfeld *et al.*, 2001). In light use efficiency (LUE) algorithms (e.g. Goetz *et al.*, 1999), daily absorbed photosynthetically active radiation (APAR) is derived from satellite-based estimates of incident PAR ( $\downarrow$ PAR) and the fraction of  $\downarrow$ PAR absorbed by the vegetation canopy ( $f_{\text{APAR}}$ ). APAR is then multiplied by  $\epsilon_g$  at the daily time step to estimate GPP.  $\epsilon_g$  is usually varied depending on biome type and/or environmental stressors (Landsberg & Waring, 1997). The Land Science Team for the Moderate Imaging Spectroradiometer (MODIS) is currently producing an 8-day GPP and an

Correspondence: David P. Turner, Department of Forest Science, Oregon State University, Corvallis, OR 97331-7501, USA, fax +541 737 1393, e-mail: david.turner@oregonstate.edu

annual NPP at the 1 km spatial resolution for the global terrestrial surface using this general scheme (Running *et al.*, 2000). A key uncertainty in these applications is the spatial and temporal variation in daily  $\epsilon_g$  (Goetz & Prince, 1999; Turner *et al.*, 2002).

Eddy covariance (EC) flux towers offer the opportunity for estimating APAR and GPP, hence  $\epsilon_g$ , at spatial and temporal scales relevant to the satellite-based scaling algorithms (Ruimy *et al.*, 1996). The spatial scale of an EC tower is the tower footprint ( $\sim 1 \text{ km}^2$ ) and the temporal scale is integration at half hourly intervals with subsequent summation to the daily time step. APAR is measured with above and below canopy PAR sensors and GPP is estimated by subtracting an estimate of ecosystem respiration from the measurement of net ecosystem exchange during the daylight hours (Goulden *et al.*, 1996a). The concurrent measurement of meteorological variables such as temperature and vapor pressure, as well as water balance variables including evapotranspiration and soil water status, can be used to understand controls on daily  $\epsilon_g$ . A network of EC towers now includes a wide range of biomes (Baldocchi *et al.*, 1996) and, more recently, successional stages within biomes (Law *et al.*, 2001).

The objective of this study was to examine the relationship of daily GPP to daily APAR over the growing season at four flux tower sites representing different biomes. Relationships of  $\epsilon_g$  to  $\downarrow\text{PAR}$ , APAR, vapor pressure deficit, and daily maximum temperature were studied to assess their relative importance in different biomes. Results were considered in relation to design of algorithms for satellite-based monitoring global NPP.

## Methods

### Sites

Four sites were included in the study (Table 1). The AGRO site is a cornfield in an agricultural setting in the

American Midwest. The KONZ site is at the Konza Long Term Ecological Research (LTER) station in the Great Plains region of the central US and is dominated by tall-grass prairie. The Harvard Forest LTER site in the northeastern US (HARV) represents the northern hardwoods biome. The NOBS site is in the boreal forest biome in northern Manitoba, Canada. Detailed information on the vegetation, climate, and soils at these sites is available at the AmeriFlux Internet site (AmeriFlux, 2001). These sites are participating in a project specifically designed to develop GPP and NPP data layers for comparison with the MODIS, GPP and NPP products (Reich *et al.*, 1999b).

### Gross primary production

Calculation of daily GPP efficiency requires estimates of GPP and of APAR.

$$\epsilon_g (\text{gC MJ}^{-1}) = \text{GPP}/\text{APAR} \quad (1)$$

where GPP is gross primary production ( $\text{gC m}^{-2} \text{d}^{-1}$ ) and APAR = absorbed PAR ( $\text{MJ m}^{-2} \text{d}^{-1}$ ). Gross primary production (GPP) estimates were derived from micrometeorological flux measurements of net ecosystem exchange (NEE) at each site. The micrometeorological methods are described for AGRO at the AmeriFlux Internet site (AmeriFlux, 2001), for KONZ in Ham & Knapp (1998), for HARV in Wofsy *et al.* (1993), and for NOBS in Goulden *et al.* (1997). Eddy covariance analysis was used at all sites except KONZ where the eddy accumulation technique was used. GPP was calculated as:

$$\text{GPP} = \text{NEE} - R_e \text{ during daylight periods} \quad (2)$$

where NEE = net ecosystem exchange ( $\mu\text{mol m}^{-2} \text{s}^{-1}$ ),  $R_e$  = ecosystem respiration ( $\mu\text{mol m}^{-2} \text{s}^{-1}$ ).

In this sign convention, the flux from the surface to the atmosphere is negative.

$R_e$  was estimated at the AGRO, HARV, and NOBS sites from the relationships of half hourly NEE at night to air

**Table 1** Name, location, dominant vegetation, year of micrometeorological observations, GPP measurement interval (day of year), and measurement days in interval for the study sites

Site	Lat./Long.	Dominant vegetation	Year	Measurement interval	Measurement days
AGRO	40.0066°N 88.2910°W	Corn	1999	154–250	96
KONZ	39.0823°N 96.5602°W	Tallgrass prairie	1997	122–279	152
HARV	42.5382°N 72.1714°W	Mixed conifer/deciduous forest	2000	120–300	180
NOBS	55.8795°N 98.4808°W	Boreal conifer forest	1997	101–290	146

temperature during periods above a threshold friction velocity (Goulden *et al.*, 1996a,b; 1997). At KONZ,  $R_e$  was estimated by scaling soil respiration and above-ground autotrophic respiration based on chamber measurements and temperature data (Ham & Knapp, 1998). Thus, daytime air temperatures strongly influenced  $R_e$  estimates. Gross primary production (GPP) was calculated for each day of the growing season for which flux data were available and estimated APAR (see below) was greater than  $0.5 \text{ MJ m}^{-2} \text{ d}^{-1}$ . Short gaps in NEE were filled in where possible following Falge *et al.* (2001), however, some multiple day gaps remained because of equipment failures.

The reliance of the GPP estimates on effective modeling of daytime  $R_e$  introduces significant uncertainties. Variations in the threshold friction velocity used for screening out periods of low turbulence at night results in variations in  $R_e$  estimates (e.g. Barford *et al.*, 2001). Underestimation of  $R_e$  is associated with possible nighttime advective flow that is not detected by the EC approach (Massman & Lee, 2002). There is also an issue with the assumption of similar temperature adjusted foliar respiration ( $R_f$ ) rates at night and during the day.  $R_f$  rates indicated by photosynthetic light response curves can be lower than foliar dark respiration (Villar *et al.*, 1995). On the other hand, temperature adjusted nighttime  $R_f$  rates may be lower than daytime rates (Hubbard *et al.*, 1995), perhaps because of depletion of labile substrates. The contribution of the  $R_e$  term to daily GPP was small at the AGRO site, intermediate at the HARV and NOBS sites, and relatively large at the KONZ site (Fig. 1). The importance of the uncertainties in  $R_e$  estimation thus varies widely and continued progress in assessing these issues will be based on intensive site-level studies as well as cross-site synthesis.

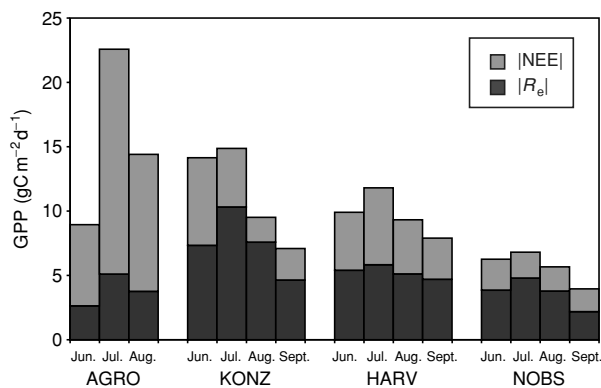


Fig. 1 The contribution of net ecosystem exchange (NEE) and ecosystem respiration ( $R_e$ ) to mean daily gross primary production (GPP) by month at each site.

## APAR

APAR was derived from measurements of solar short wave radiation or PAR, which were summed over a day ( $\downarrow\text{PAR}$ ) and multiplied by estimates of  $f_{\text{APAR}}$ . At NOBS and HARV,  $\downarrow\text{PAR}$  was measured with a quantum sensor at the top of the EC tower and half hourly means were recorded. The data are available at the AmeriFlux Internet site (AmeriFlux, 2001). At AGRO,  $\downarrow\text{PAR}$  was measured with a quantum sensor at a station in the SURFRAD network, which was within 5 km of the EC tower (SURFRAD, 2001). At KONZ, short wave radiation was measured at the Konza Long-term Ecological Research (LTER) station within 5 km of the tower (Konza, 2001). In cases of missing  $\downarrow\text{PAR}$  data, daily minimum and maximum temperature were used to estimate daily  $\downarrow\text{PAR}$  following Thornton & Running (1999).

Estimates of  $f_{\text{APAR}}$  were derived from seasonal trajectories of leaf area index (LAI) using a simple relationship between LAI and  $f_{\text{APAR}}$  based on the Beer–Lambert Law (Jarvis & Leverenz, 1983):

$$\text{LAI} = (-1/K) \ln(I_z/I_0), \quad (3)$$

where  $I_z$  = below canopy PAR,  $I_0$  = incoming PAR ( $\downarrow\text{PAR}$ ) and  $K$  = radiation extinction coefficient.

Ignoring canopy reflection, which is relatively low (Gower *et al.*, 1999),  $f_{\text{APAR}}$  is then derived as:

$$f_{\text{APAR}} = 1 - (I_z/I_0),$$

where  $I_z/I_0 = e^{(\text{LAI}(-K))}$ .

At NOBS, evergreen conifers dominate the vegetation and the LAI from Gower *et al.* (1997) was assumed constant year round. This approach probably produces an overestimate of canopy  $f_{\text{APAR}}$  at NOBS because of the columnar arrangement of the foliage on the black spruce trees. However, much of the transmitted PAR is absorbed in any case by the bryophyte layer on the ground and the bryophytes contributed significantly to GPP (Goulden & Crill, 1997). At HARV, above and below canopy measurements of PAR were used with (Eqn 3) to derive a weekly LAI. At AGRO, monthly measurements of LAI were made in 1999 (Campbell *et al.*, 1999) and daily estimates were available based on reflectance measurements at the EC tower (AmeriFlux, 2001; Turner *et al.*, 2002). The seasonal LAI trajectory for KONZ was from periodic measurements made in 1997 (Bremer & Ham, 1999). Values of  $K$  were approximated as 0.4 for KONZ (Massman, 1992), 0.46 for AGRO (Daughtry *et al.*, 1992), and 0.5 at the other sites (Jarvis & Leverenz, 1983). PAR absorbed by below canopy vegetation such as early spring herbs at HARV was not included in the analysis.

### Analysis of $\epsilon_g$

To make comparisons across sites, GPP and APAR data for the period June 1 to September 30 were used. The temporal constraint criteria served to eliminate days early and late in the growing season when uncertainties in APAR and GPP were greatest. Linear and rectangular hyperbola response curves (Ruimy *et al.*, 1995) were fit to the plots of GPP against APAR. Mean daily  $\epsilon_g$  was compared across months within a site, and for all months across sites. The month of September at AGRO was omitted from the  $\epsilon_g$  comparisons because the foliage was rapidly changing from green to brown (Gallo *et al.*, 1993). Relationships of  $\epsilon_g$  to  $\downarrow$ PAR, APAR, daytime average vapor pressure deficit (VPD), and maximum daily temperature ( $T_{\max}$ ) were assessed within each site across the growing season. The VPD and  $T_{\max}$  data were from the same sources as the  $\downarrow$ PAR data.

## Results and Discussion

### Daily $\downarrow$ PAR, LAI, and GPP

The plots of  $\downarrow$ PAR against DOY showed expected patterns across the year associated with solar-surface

geometry, and strong day-to-day variation associated with weather events (Fig. 2). Maximum daily  $\downarrow$ PAR over the growing season reached approximately  $14 \text{ MJ d}^{-1}$  for all sites. At HARV, the summertime values tended to be lower than the maximum value because of recurrent cloudiness and/or a greater optical depth of the atmosphere.

The maximum values and the seasonal LAI trajectories (Fig. 3) differed widely among the biomes. The highest LAIs were measured in the agricultural field and the lowest at the tallgrass prairie. The forested sites had intermediate LAIs of about 4. These values are generally consistent with earlier measurements of LAI in these biomes (Gallo *et al.*, 1985; Schimel *et al.*, 1991; Amthor *et al.*, 1994; Chen & Cihlar, 1996).

The maximum daily GPP was relatively low at NOBS, reaching only  $8 \text{ gC m}^{-2} \text{ d}^{-1}$ , compared with values of 14 for HARV, 18 for KONZ, and 27 for AGRO (Fig. 4). All sites showed a symmetrical seasonal pattern in GPP that tracked the seasonal trend in  $\downarrow$ PAR. Day to day variation in GPP was not as great as the variation in  $\downarrow$ PAR. The beginning of the measured GPP was significantly delayed at AGRO compared to the other sites, reflecting crop-planting dates in May.

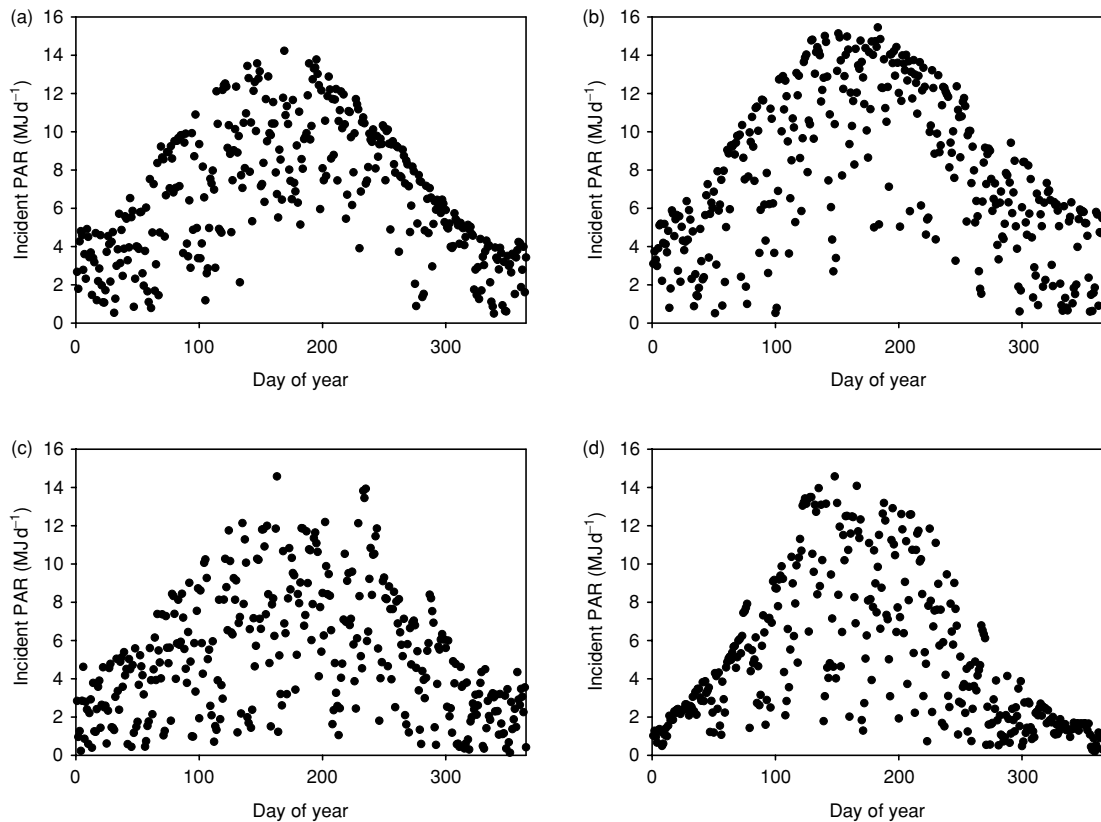


Fig. 2 Daily incident photosynthetically active radiation ( $\downarrow$ PAR) at each site (a = AGRO, b = KONZ, c = HARV, d = NOBS).

## Daily GPP

The relationship of GPP to APAR varied widely between the sites (Fig. 5). At the AGRO, HARV and NOBS sites, a rectangular hyperbola fit gave the highest  $r^2$ , whereas at KONZ the linear fit was as good as the rectangular hyperbola. The nonlinear relationships suggest the

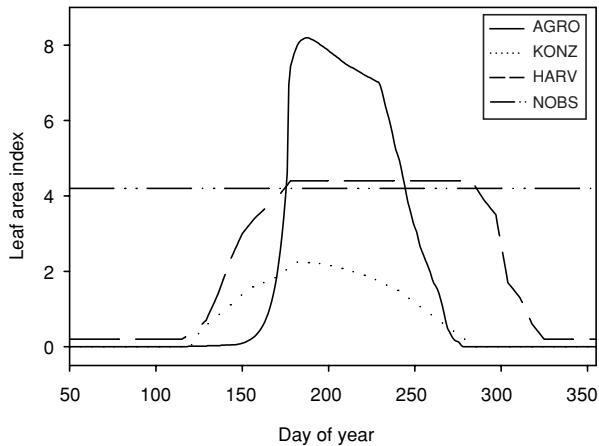


Fig. 3 The seasonal trajectory for canopy leaf area index at each site.

possibility of overestimating GPP using an LUE algorithm if the  $\varepsilon_g$  were based on data with low APAR.

Saturation of net photosynthesis with increasing photosynthetic photon flux density (PPFD), hence non-linearity in the relationship, is commonly observed at the leaf-level with cuvette measurements (e.g. Teskey *et al.*, 1994). At the canopy scale, short-term estimates of gross canopy photosynthesis from eddy covariance measurements over a range of solar radiation regimes have also found saturation to some degree (Ruimy *et al.*, 1995), as indicated by a hyperbolic fit of canopy  $\text{CO}_2$  uptake to PPFD under conditions of high  $f_{\text{APAR}}$ . Theoretically, the hyperbolic relationship would be most expected under conditions of low LAI or low photosynthetic capacity (Baldocchi & Amthor, 2001). A trend towards linearity would be expected at high LAIs because mutual shading results in more of the foliage operating in the linear part of the leaf-level light response curve (Teskey *et al.*, 1995).

GPP at the daily time step integrates periods of high and low PPFD, and thus nonlinearity in the daily APAR–GPP relationship is likely to be moderated relative to short-term leaf-level and canopy-level light response curves. Leuning *et al.* (1995) found a nearly linear relationship of daily-simulated canopy photosynthesis to daily incident PPFD using a short time step, multilayer

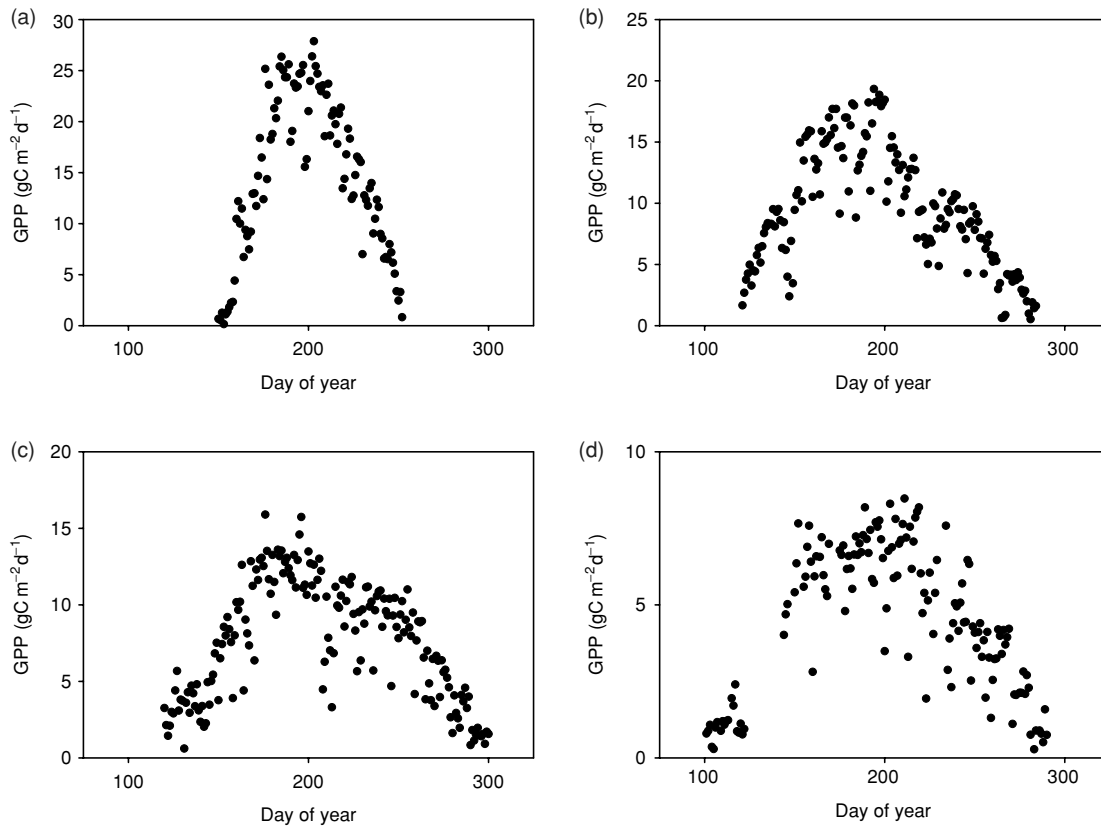
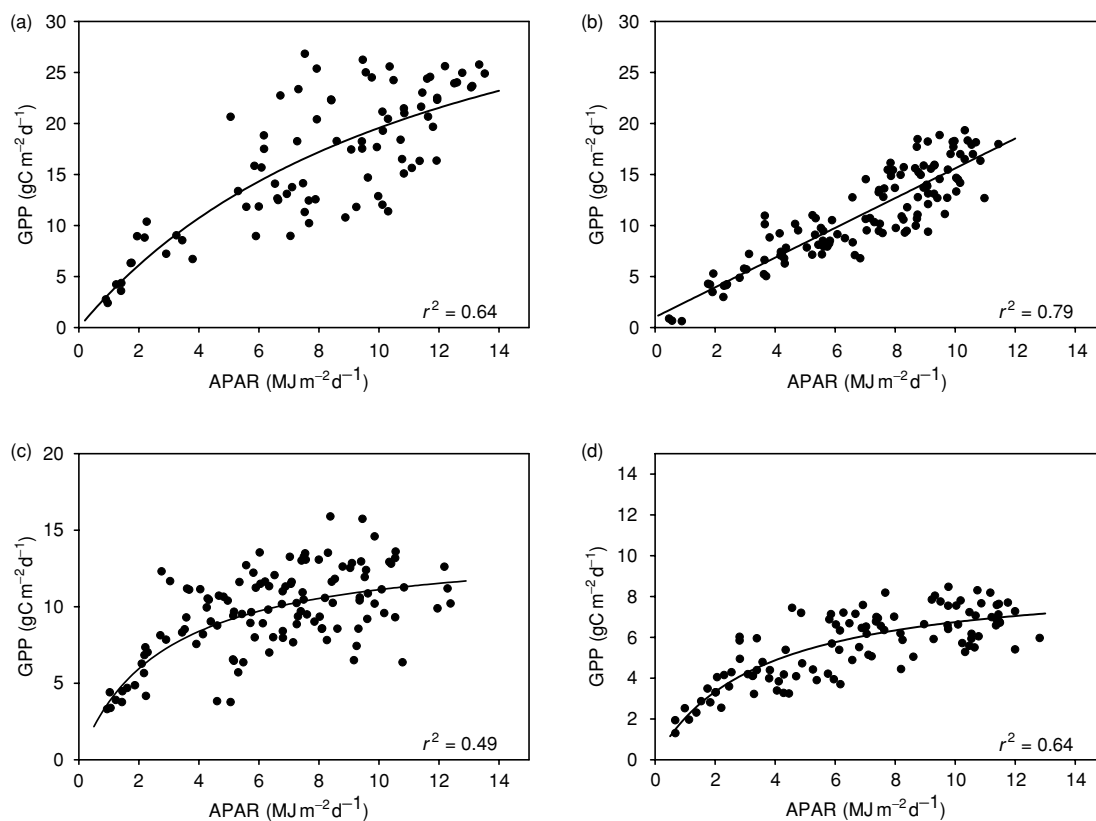


Fig. 4 Daily gross primary production (GPP) for one year at each site (a = AGRO, b = KONZ, c = HARV, d = NOBS).



**Fig. 5** The relationship of gross primary production (GPP) to absorbed photosynthetically active radiation (APAR) at each site. The KONZ plot is linear and the others are rectangular hyperbolas (a = AGRO, b = KONZ, c = HARV, d = NOBS).

canopy photosynthesis model. The strong linear relationship of GPP to APAR at the grassland site in this study is consistent with this interpretation.

Nevertheless, as is evident from this study and others (Williams *et al.*, 1998; Oechel *et al.*, 2000), there may remain a hyperbolic relationship of GPP to  $\downarrow$ PAR, and more specifically APAR, at the daily time step. The two-forested sites showed the strongest nonlinearity in their relationships of GPP to APAR. At a boreal forest site, photosynthetic capacity of the conifers (Woodward & Smith, 1994) and mosses (Green & Lange, 1994) is relatively low, which would lead to saturation and the observed nonlinear relationship. In a branch chamber study with black spruce (*Picea mariana* (Mill.) BSP), the dominant conifer species at the NOBS site, the upper bound of carbon uptake per unit leaf area per day was also hyperbolically related to the daily sum of  $\downarrow$ PAR (Rayment & Jarvis, 1999). At the deciduous forest site, the photosynthetic capacity of the tree species is higher than in the boreal forests (Woodward & Smith, 1994). In addition, the LAI is relatively high and the leaves in the dominant deciduous species tend towards random distribution in space and spherical distribution of leaf inclination angles (Norman & Campbell, 1989). These features

would favor penetration of sunlight deep into the canopy and in principle promote a linear relationship. However, shade leaves have relatively low photosynthetic capacity (Ellsworth & Reich, 1993) and high APAR days may be associated with feedback inhibition of photosynthesis in the afternoon (Amthor *et al.*, 1994), both of which would reduce GPP relative to APAR.

#### *Annual and monthly $\epsilon_g$*

Mean daily  $\epsilon_g$  over the June to September period was lowest at the boreal forest site, highest at the agricultural site, and intermediate at the grassland and hardwood forest sites (Table 2). This pattern is generally consistent with differences among the biomes in net primary production (Saugier *et al.*, 2001) and in light use efficiency for net primary production (Gower *et al.*, 1999). The season average  $\epsilon_g$  at AGRO is low relative to what would be expected based on light use efficiency for net primary production in corn (Sinclair & Horie, 1989; Major *et al.*, 1991), which suggests a possible underestimation of night-time fluxes (hence ecosystem respiration and daytime GPP) with the EC approach. At Konza, the mean daily  $\epsilon_g$  value is close to the daily values derived from

chamber studies near the EC tower site (Norman *et al.*, 1991). At NOBS, the annual GPP from Ryan *et al.* (1997) divided by the annual APAR from this study gives an  $\epsilon_g$  of  $0.8 \text{ gCMJ}^{-1}$ , close to the  $1.0 \text{ gCMJ}^{-1}$  for June to September in this study. The relatively low value at NOBS is also consistent with the inverse relationship of  $\epsilon_g$  to mean annual temperature among 9 forest sites reported by Lafont *et al.* (2002). The low nitrogen availability in boreal forests and relatively high nitrogen availability in agricultural fields have a strong influence on the relative  $\epsilon_g$  values among biomes.

Besides, differences in mean daily  $\epsilon_g$ , the sites differed in how  $\epsilon_g$  varied over the growing season. The strongest seasonal pattern was at AGRO where the decline in  $\epsilon_g$  after day 200 was closely related to a decline in foliar nitrogen concentration (Fig. 6). Other studies of light use efficiency in corn have reported similar trends (Tollenaar & Bruulsema, 1988). At KONZ,  $\epsilon_g$  decreased significantly in the month of August, but recovered late in the growing season. The tallgrass prairie is sensitive to soil drought (Knapp *et al.*, 2001) and the volumetric soil water content at the KONZ site in 1997 hit a seasonal low around DOY 220 (Bremer & Ham, 1999) which corresponds to the period of relatively low  $\epsilon_g$ . Drought related decline in  $\epsilon_g$  is also evident in short grass prairie (Nouvellon *et al.*, 2000).

The effect of seasonality on  $\epsilon_g$  was also evident at the NOBS site, which showed an increase in  $\epsilon_g$  between June

and August (Table 2). That observation is consistent with the EC flux measurements at another boreal forest flux tower site where a seasonal cycle in the initial slope of the rectangular hyperbola fit of PPFD and canopy flux was evident (Hollinger *et al.*, 1999). The changing solar zenith angle, hence improved penetration of sunlight into the canopy, may in part account for this trend (Gu *et al.*, 1999) but seasonality in light saturated photosynthesis in boreal conifer species has also been observed (Middleton *et al.*, 1997; Rayment & Jarvis, 1999). Leaf-level measurements at HARV show a consistent light saturated photosynthesis in July and August but a decline in that parameter between August and September (Bassow & Bazzaz, 1998). The decrease in  $\epsilon_g$  from August to September in this study was relatively small but the change was in the expected direction. Some species at Harvard Forest show a significant early season lag in achieving maximum photosynthetic capacity (Morecroft & Roberts, 1999) but that effect may not have been resolved in this analysis because it did not include May.

#### Daily $\epsilon_g$

Within months,  $\epsilon_g$  decreased with increasing  $\downarrow\text{PAR}$  and APAR at all sites (APAR relationships are shown in Fig. 7). The  $\downarrow\text{PAR}$  and APAR relationships were similar because  $f_{\text{APAR}}$  was generally high during the June–September period. The slopes of the monthly linear relationships of  $\epsilon_g$  to APAR were most negative at the hardwood forest site. For all sites the decline of  $\epsilon_g$  with increasing APAR was strongest in mid summer: for the month of July, an  $r^2$  between 0.65 and 0.89 for the least squares regression linear fit was observed at each site, with  $\epsilon_g$  generally varying by nearly a factor of 3 during the month (Fig. 7). At the agricultural site, the slope was appreciably less negative in August than in July.

The relationships of  $\epsilon_g$  to APAR reflect in part, the nonlinear relationships of GPP to APAR (Fig. 5). If the

**Table 2** Light use efficiency for gross primary production ( $\epsilon_g \text{ gCMJ}^{-1}$ ) during the growing season. Values are means of daily  $\epsilon_g$  with standard deviations in parentheses

Site	June	July	August	September	June–September
AGRO	2.3 (0.6)	2.4 (0.6)	1.7 (0.4)	–	2.2 (0.7)
KONZ	1.7 (0.2)	1.8 (0.4)	1.4 (0.3)	1.9 (0.5)	1.7 (0.4)
HARV	1.9 (1.0)	1.8 (0.6)	1.8 (0.8)	1.6 (0.7)	1.8 (0.8)
NOBS	0.8 (0.3)	1.0 (0.4)	1.2 (0.6)	1.2 (0.5)	1.0 (0.5)

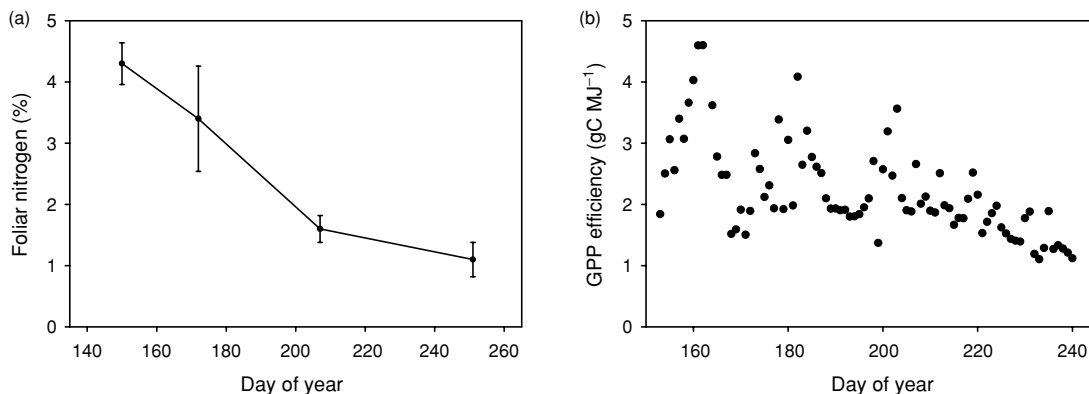


**Fig. 6** Foliar nitrogen concentration and GPP efficiency at the AGRO site 1999. Foliar nitrogen data are from ORNL (2001).

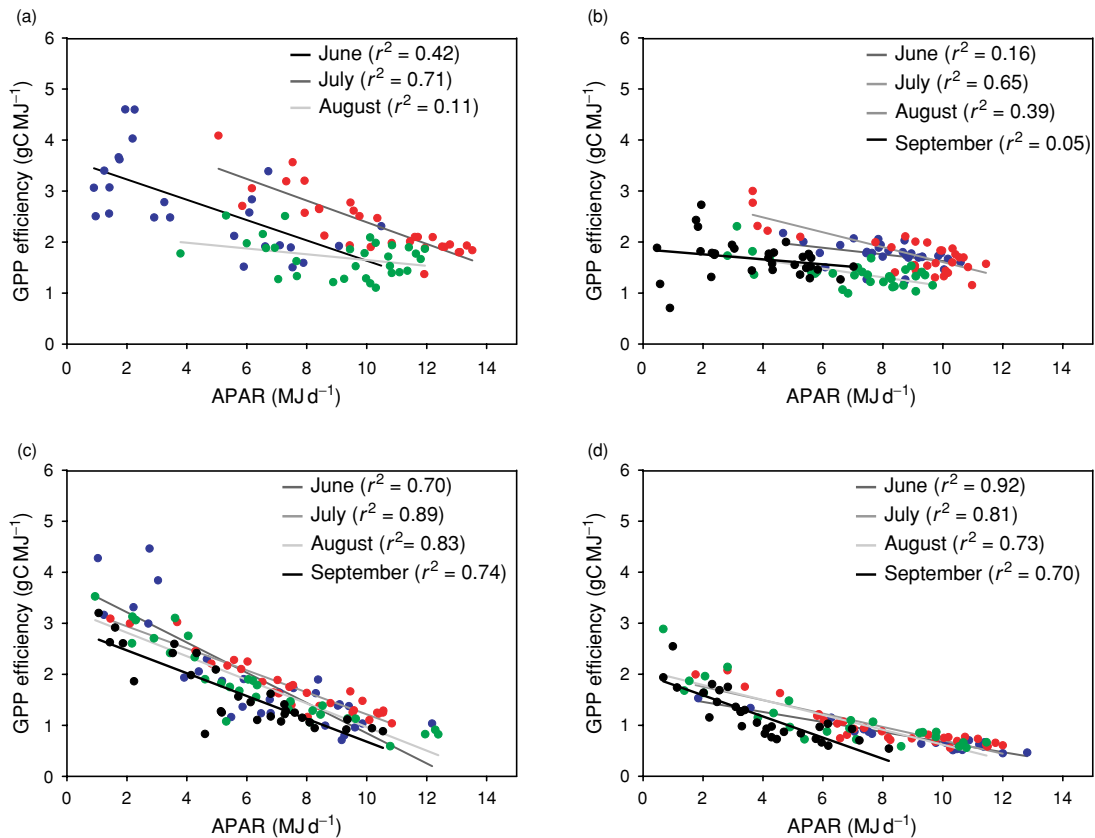


**Fig. 7** The relationship of light use efficiency for gross primary production ( $\epsilon_g$ ) to absorbed photosynthetically active radiation (APAR) at each site (a = AGRO, b = KONZ, c = HARV, d = NOBS). The plots are linear fits for each month.

canopy is light saturated for a significant proportion of the day on high APAR days, the daily  $\epsilon_g$  will come down. These relationships are also related to canopy-level observations that photosynthesis per unit PPFD is higher under overcast skies, when PPFD is relatively low, than under clear skies (Rochette *et al.*, 1996). This mechanism would tend to raise  $\epsilon_g$  at low to mid APAR values.

An increased efficiency at low  $\downarrow$ PAR is believed to be an effect of lower leaf temperature, lower leaf to air VPD, and a more uniform distribution of irradiance under overcast conditions (Lloyd *et al.*, 1995). Goulden *et al.* (1997) observed higher photosynthesis per unit PPFD under cloudy compared to sunny conditions, and similar observations of GPP or net ecosystem exchange have been made at other tower sites (Hollinger *et al.*, 1994; Fan *et al.*, 1995; Freedman *et al.*, 2001; Law *et al.*, 2002). There was a positive relationship of  $\epsilon_g$  to cloudiness in July in the four datasets used in this study (Fig. 8), with relatively shallow slopes at KONZ and NOBS compared to HARV and AGRO. At the grassland vegetation site, erectophile leaves that promote an even distribution of radiation throughout the canopy may reduce the difference between  $\epsilon_g$  on clear and overcast days. At NOBS, the

photosynthetic rates are quite low to begin with (Middleton *et al.*, 1997) and responses to variation in the light environment may be modest relative to more productive ecosystems.

VPD tends to be positively correlated with  $\downarrow$ PAR and APAR (e.g., Fig. 9) because clear days with high  $\downarrow$ PAR are also likely to have high temperatures and VPD. There was a weak inverse relationship of  $\epsilon_g$  to VPD at all sites (i.e.  $r^2$  always < 0.30, plots not shown) but VPD was probably not the critical factor. The strength of the decline in  $\epsilon_g$  with increasing APAR was not diminished when data were screened for days with average VPD < 750 Pa. Leaf-level studies at Harvard Forest and canopy studies at other deciduous forest sites have indicated relatively weak effects of VPD on photosynthesis in most cases (Baldocchi *et al.*, 1987; Bassow & Bazzaz, 1998), which is consistent with the lack of a relationship at the canopy scale seen in this study. Eddy flux evaluations of canopy photosynthesis in relation to VPD in boreal forests have also not indicated much sensitivity (Goulden *et al.*, 1997; Jarvis *et al.*, 1997). Generally, crop and grasslands are short and dense, thus tending to be decoupled from the atmosphere and also relatively unresponsive to VPD (Jarvis & McNaughton, 1986).



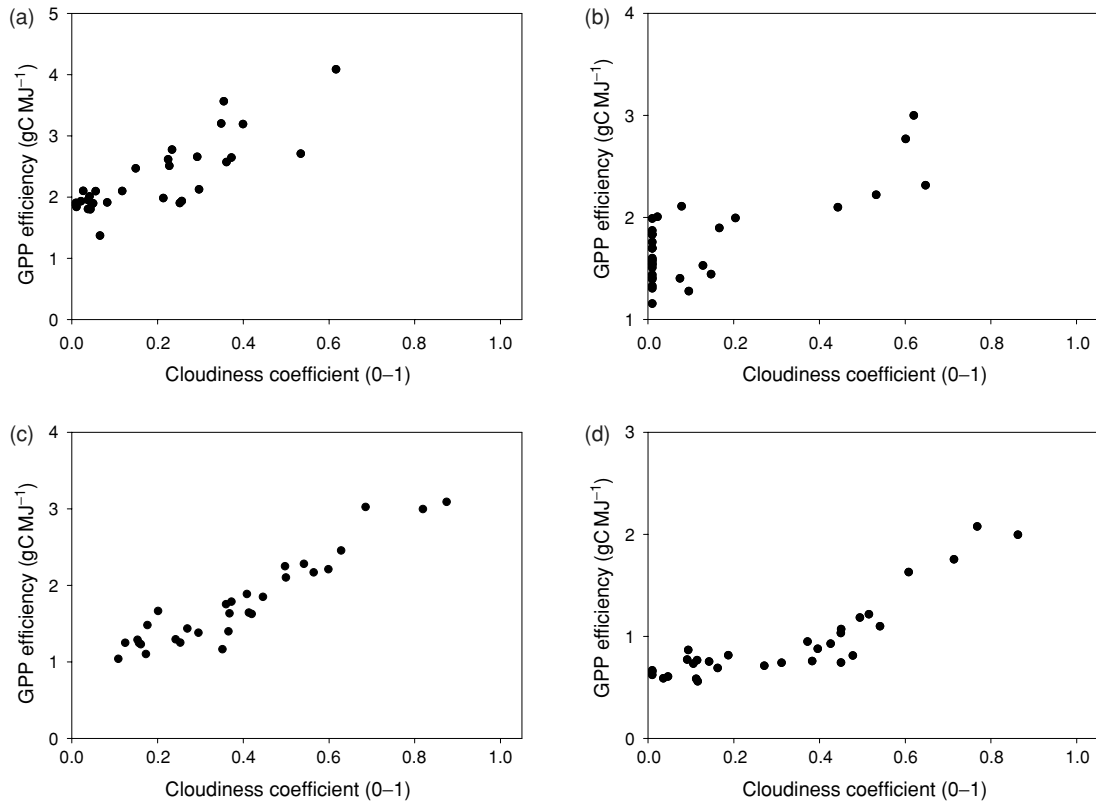


**Fig. 8** Site-specific relationships of light use efficiency for gross primary production ( $\epsilon_g$ ) to cloudiness in July (a = AGRO, b = KONZ, c = HARV, d = NOBS). The cloudiness coefficient is equal to 1 minus the ratio of observed photosynthetically active radiation (PAR) to clear sky PAR. The clear sky condition was modeled following Thornton & Running (1999).

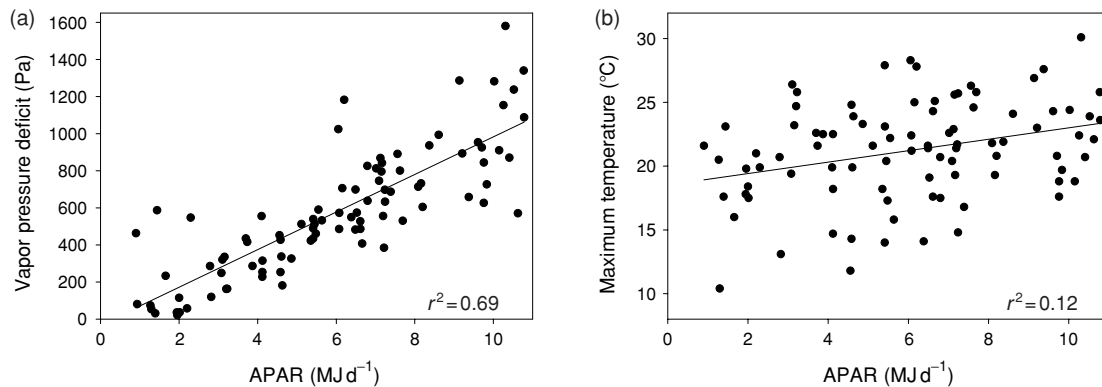


**Fig. 9** The relationship of (a) vapor pressure deficit (VPD) to absorbed photosynthetically active radiation (APAR), and (b) daily maximum temperature to APAR for the June to September period at Harvard Forest.

Daily maximum temperature also covaries with APAR (e.g. Fig. 9), so again there was a weak inverse relationship of  $\epsilon_g$  to  $T_{\max}$  ( $r^2 < 0.10$  at all sites, data not shown). At the temperate zone sites, temperatures during June through September did not often extend to the high or low values where strong negative effects would be expected (Mebrahtu *et al.*, 1991; Teskey *et al.*, 1995). The

results were consistent with earlier leaf-level measurements at the KONZ and HARV sites that did not find strong temperature effects on photosynthesis during this part of the growing season (Polley *et al.*, 1992; Bassow & Bazzaz, 1998). EC measurements of half hourly GPP at NOBS found a positive relationship to air temperature over the May 1 to October 31 period (Goulden *et al.*, 1997)

suggesting significant temperature effects in the colder months of May and October. Low temperatures in April clearly inhibit photosynthesis in boreal forests because of frozen soils and physiological constraints (Larcher, 1995; Goulden *et al.*, 1997).

#### *Implications for development of LUE algorithms*

Regular global monitoring of terrestrial GPP and NPP based on LUE approaches has now begun and results will be of continuing interest with regard to mapping spatial patterns in carbon flux and understanding inter-annual variation in the global carbon cycle.  $\epsilon_g$  is a critical component of the LUE algorithms and a variety of approaches to estimating  $\epsilon_g$  at a daily time step over gridded areas ranging from the regional to the global scale have been implemented (Goetz *et al.*, 1999; Oechel *et al.*, 2000; Running *et al.*, 2000; Williams *et al.*, 2001). Until recently, opportunities for calibration and validation of  $\epsilon_g$  have been limited.

Results of this and other studies suggest that biomes differ significantly with respect to the maximum daily  $\epsilon_g$ . Remote sensing has proved effective in mapping vegetation cover, both in terms of biome types (Loveland *et al.*, 1991) and stages of succession (Cohen *et al.*, 1995), which may also differ in  $\epsilon_g$  (Chen *et al.*, 2002). Thus the simultaneous classification of land cover and estimation of  $f_{\text{APAR}}$  by remote sensing provides a strong basis for an LUE algorithm. Recent synthesis efforts have revealed that fundamental vegetation properties such as photosynthetic capacity covary with leaf traits such as leaf thickness (Enriquez *et al.*, 1996; Reich *et al.*, 1999a). These observations suggest that to the degree remote sensing is able to detect these traits (e.g. Pierce *et al.*, 1994) spatially continuous mapping of photosynthetic capacity with remote sensing without recourse to classification may ultimately be possible.

Effects of daily weather on  $\epsilon_g$  are also clearly important. Most commonly, LUE algorithms employ temperature and VPD scalars that are adjusted downward as stress increases (Goetz *et al.*, 1999; Running *et al.*, 2000). In this study these variables were not strong correlates of daily  $\epsilon_g$  however, they may play a stronger role in regulating  $\epsilon_g$  elsewhere. An observation from this study that is generally not used in LUE algorithms is the decline in daily  $\epsilon_g$  with increasing  $\downarrow\text{PAR}$  or APAR. The relationship appears to be quite general, although the magnitude of the effect is related to the structural properties of the canopy and the productive capacity of the vegetation. A simple function for the effect could potentially be formulated from maximum  $\epsilon_g$ ,  $\downarrow\text{PAR}$ , and  $f_{\text{APAR}}$ . If used in an LUE algorithm (e.g. Lafont *et al.*, 2002), it would in theory prevent overestimation of GPP under clear sky

conditions or – depending on how maximum  $\epsilon_g$  was parameterized – underestimation on cloudy days.

Flux tower studies also suggest that  $\epsilon_g$  changes with time in the growing season. The day of year is readily tracked for use in an LUE algorithm but an important research issue is an improved understanding of the climatic triggers influencing phenology and photosynthetic capacity (Dougherty *et al.*, 1994; White *et al.*, 1997; Botta *et al.*, 2000). Data assimilation approaches that use satellite-based observations to update a general circulation model are beginning to generate relevant weather data fields (DAO, 2002), and these data could be employed to drive phenology algorithms (e.g. Kaduk & Heimann, 1996).

#### Conclusions

Improving operational LUE algorithms for monitoring global GPP and NPP is desirable in the context of efforts to understand trends in the global carbon budget and to monitor global NPP. Observations at eddy covariance flux towers are made at a spatial and temporal scale relevant to characterizing daily  $\epsilon_g$  and its response to environmental and seasonal variation. Results here suggest differences among biomes in maximum and growing season average  $\epsilon_g$ , in temporal patterns in the variation of  $\epsilon_g$ , and in the degree to which  $\epsilon_g$  declines at high APAR. More comprehensive surveys of flux tower observations could provide near real time and long-term information for calibration and validation of globally applied  $\epsilon_g$  algorithms.

#### Acknowledgements

This study was funded by NASA through the Terrestrial Ecology Program. Funding at individual tower sites was provided by the Department of Energy (HARV, NOBS, KONZ) and NOAA (AGRO). Thanks to Alan Knapp (Kansas State University) for scaling ecosystem respiration at the KONZ site. Special thanks to all the scientists and support staff at the four flux towers. Site coordinators are Tilden Meyers (NOAA) at AGRO, S. Wofsy (Harvard University) at NOBS and HARV, and Jay Ham (Kansas State University) at KONZ. Data available through AmeriFlux, FLUXNET and the ORNL DAAC Mercury Data System were essential to this study.

#### References

- AmeriFlux (2001) <http://public.ornl.gov/ameriflux/Participants/Sites/Map/index.cfm>.
- Amthor JS, Goulden ML, Munger JW *et al.* (1994) Testing a mechanistic model of forest-canopy mass and energy exchange using eddy correlation: carbon dioxide and ozone uptake in a mixed oak-maple stand. *Australian Journal of Plant Physiology*, **21**, 623–651.
- Baldocchi DD, Amthor JS (2001) Canopy photosynthesis: history, measurements, and models. In: *Terrestrial Global Productivity*

- (eds Roy J, Saugier B, Mooney HA), pp. 9–31. Academic Press, San Diego.
- Baldocchi D, Valentini R, Running S *et al.* (1996) Strategies for measuring and modeling carbon dioxide and water vapour fluxes over terrestrial ecosystems. *Global Change Biology*, **2**, 159–168.
- Baldocchi DD, Verma SB, Anderson DE (1987) Canopy photosynthesis and water use efficiency in a deciduous forest. *Journal of Applied Forestry*, **24**, 251–260.
- Barford CC, Wofsy SW, Goulden ML *et al.* (2001) Factors controlling long- and short-term sequestration of atmospheric CO<sub>2</sub> in a mid-latitude forest. *Science*, **294**, 1688–1691.
- Bassow SL, Bazzaz FA (1998) How environmental conditions affect canopy leaf-level photosynthesis in four deciduous tree species. *Ecology*, **79**, 2660–2675.
- Behrenfeld MJ, Randerson JT, McClain CR *et al.* (2001) Biospheric production during an ENSO transition. *Science*, **291**, 2594–2597.
- Botta A, Viovy N, Cias P *et al.* (2000) A global prognostic scheme of leaf onset using satellite data. *Global Change Biology*, **6**, 709–726.
- Bremer DJ, Ham JM (1999) Effect of spring burning on the surface energy balance in a tallgrass prairie. *Agricultural and Forest Meteorology*, **97**, 43–54.
- Campbell JL, Burrows S, Gower ST *et al.* (1999) *BigFoot: Characterizing Land Cover, LAI, and NPP at The Landscape Scale for EOS/MODIS Validation*. Field Manual, Version 2.1. 1999. Environmental Sciences Division, Oak Ridge National Laboratory, Oak Ridge, TN.
- Chen JM, Cihlar J (1996) Retrieving leaf area index of boreal conifer forests using Landsat TM images. *Remote Sensing of Environment*, **55**, 153–162.
- Chen J, Falk M, Euskirchen E *et al.* (2002) Biophysical controls of carbon flows in three successional Douglas-fir stands based on eddy-covariance measurements. *Tree Physiology*, **22**, 169–177.
- Cohen WB, Spies TA, Fiorella M (1995) Estimating the age and structure of forests in a multi-ownership landscape of western Oregon, USA. *International Journal of Remote Sensing*, **16**, 721–746.
- DAO (2002) NASA Data Assimilation Office. <http://dao.gsfc.nasa.gov/>.
- Daughtry CST, Gallo KP, Goward SN *et al.* (1992) Spectral estimates of absorbed radiation and phytomass production in corn and soybean canopies. *Remote Sensing of Environment*, **39**, 141–152.
- Dougherty PM, Whitehead D, Vose JM (1994) Environmental influences on the phenology of pine. *Ecological Bulletins*, **43**, 64–75.
- Ellsworth DS, Reich PB (1993) Canopy structure and vertical patterns of photosynthesis and related leaf traits in a deciduous forest. *Oecologia*, **96**, 169–178.
- Enriquez S, Duarte C, Sand-Jensen K *et al.* (1996) Broad-scale comparison of photosynthetic rates across phototrophic organisms. *Oecologia*, **108**, 197–206.
- Falge E, Baldocchi D, Olson R *et al.* (2001) Gap filling strategies for defensible annual sums of net ecosystem exchange. *Agricultural and Forest Meteorology*, **107**, 43–69.
- Fan S, Goulden M, Munger ML *et al.* (1995) Environmental controls on the photosynthesis and respiration of a boreal lichen woodland: a growing season of whole-ecosystem exchange measurements by eddy correlation. *Oecologia*, **102**, 443–452.
- Field CB, Randerson JT, Malmstrom CM (1995) Global net primary production: combining ecology and remote sensing. *Remote Sensing of Environment*, **51**, 74–88.
- Freedman JM, Fitzjarrald DR, Moore KE *et al.* (2001) Boundary layer clouds and vegetation-atmosphere feedbacks. *Journal of Climate*, **14**, 180–197.
- Gallo KP, Daughtry CST, Bauer ME (1985) Spectral estimation of absorbed photosynthetically active radiation in corn canopies. *Remote Sensing of Environment*, **17**, 221–232.
- Gallo KP, Daughtry CST, Wiegand CL (1993) Errors in measuring absorbed radiation and computing crop radiation use efficiency. *Agronomy Journal*, **85**, 1222–1228.
- Goetz SJ, Prince SD (1999) Modelling terrestrial carbon exchange and storage: evidence and implications of functional convergence in light-use efficiency. *Advances in Ecological Research*, **28**, 57–92.
- Goetz SJ, Prince SD, Goward SN *et al.* (1999) Satellite remote sensing of primary production: an improved production efficiency modelling approach. *Ecological Modelling*, **122**, 239–255.
- Goulden ML, Crill PM (1997) Automated measurements of CO<sub>2</sub> exchange at the moss surface of a black spruce forest. *Tree Physiology*, **17**, 537–542.
- Goulden ML, Daube BC, Fan S-M *et al.* (1997) Physiological responses of a black spruce forest to weather. *Journal of Geophysical Research*, **102**, 28987–28996.
- Goulden ML, Munger JW, Fan S-M *et al.* (1996a) Measurements of carbon sequestration by long-term eddy covariance: methods and a critical evaluation of accuracy. *Global Change Biology*, **2**, 169–182.
- Goulden ML, Munger JW, Fan S-M *et al.* (1996b) Exchange of carbon dioxide by a deciduous forest: response to interannual climate variability. *Science*, **271**, 1576–1578.
- Gower ST, Kucharik CJ, Norman JM (1999) Direct and indirect estimation of leaf area index,  $f_{APAR}$  and net primary production of terrestrial ecosystems. *Remote Sensing of Environment*, **70**, 29–51.
- Gower ST, Vogel JG, Norman JM *et al.* (1997) Carbon distribution and aboveground net primary production in aspen, jack pine, and black spruce stands in Saskatchewan and Manitoba, Canada. *Journal of Geophysical Research*, **102**, 29029–29041.
- Green TGA, Lange OL (1994) Photosynthesis in poikilohydric plants: a comparison of lichens and bryophytes. In: *Ecophysiology of Photosynthesis* (eds Schultze E-D, Caldwell MM), pp. 319–341, Vol. 100. Springer, Berlin.
- Gu L, Fuentes JD, Shugart HH (1999) Responses of net ecosystem exchanges of carbon dioxide to changes in cloudiness: results from two North American deciduous forests. *Journal of Geophysical Research*, **104**, 31421–31434.
- Ham JM, Knapp AK (1998) Fluxes of CO<sub>2</sub>, water vapor, and energy from a prairie ecosystem during the seasonal transition from carbon sink to carbon source. *Agricultural and Forest Meteorology*, **89**, 1–14.
- Hollinger DY, Goltz SM, Davidson EA *et al.* (1999) Seasonal patterns and environmental control of carbon dioxide and water vapour exchange in an ecotonal boreal forest. *Global Change Biology*, **5**, 891–902.

- Hollinger DY, Kelliher FM, Byers JN *et al.* (1994) Carbon dioxide exchange between an undisturbed old-growth temperate forest and the atmosphere. *Ecology*, **75**, 134–150.
- Hubbard RM, Ryan MG, Lukens DL (1995) A simple, battery-operated, temperature-controlled cuvette for respiration measurements. *Tree Physiology*, **15**, 175–179.
- Jarvis PG, Leverenz JW (1983) Productivity of temperate deciduous and evergreen forests. In: *Ecosystem Processes: Mineral Cycling, Productivity, and Man's Influence* (eds Lange OL, Nobel PS, Osmond CB *et al.*), pp. 233–280. Physiological Plant Ecology, New Series, Vol. 12D. Springer, New York.
- Jarvis P, Massheder JM, Hale SE *et al.* (1997) Seasonal variation of carbon dioxide, water vapor, and energy exchanges of a boreal black spruce forest. *Journal of Geophysical Research*, **102**, 28953–28966.
- Jarvis PG, McNaughton KG (1986) Stomatal control of transpiration: scaling up from leaf to region. *Advances in Ecological Research*, **15**, 1–19.
- Kaduk J, Heimann M (1996) A prognostic phenology model for global terrestrial carbon cycle models. *Climate Research*, **6**, 1–19.
- Knapp AK, Briggs JM, Koelliker JK (2001) Frequency and extent of water limitation to primary production in a mesic temperate grassland. *Ecosystems*, **4**, 19–28.
- Konza (2001) Konza Long Term Ecological Research site. <http://www.konza.ksu.edu/>.
- Lafont S, Kergoat L, Dedieu G *et al.* (2002) Spatial and temporal variability of land CO<sub>2</sub> fluxes estimated with remote sensing and analysis data over western Eurasia. *Tellus B*, **4**, 820–833.
- Landsberg JJ, Waring RH (1997) A generalized model of forest productivity using simplified concepts of radiation-use efficiency, carbon balance, and partitioning. *Forest Ecology and Management*, **95**, 209–228.
- Larcher W (1995) *Physiological Plant Ecology*. Springer, Berlin, 506pp.
- Law BE, Falge E, Gu L *et al.* (2002) Environmental controls over carbon dioxide and water vapor exchange of terrestrial vegetation. *Agricultural and Forest Meteorology*, **113**, 97–120.
- Law BE, Thornton PE, Irvine J *et al.* (2001) Carbon storage and fluxes in ponderosa pine forests at different developmental stages. *Global Change Biology*, **7**, 1–23.
- Leuning R, Kelliher M, DePury DGG *et al.* (1995) Leaf nitrogen, photosynthesis, conductance and transpiration: scaling from leaves to canopies. *Plant, Cell and Environment*, **18**, 1183–1200.
- Lloyd J, Wong SC, Styles JM *et al.* (1995) Measuring and modelling whole-tree gas exchange. *Australian Journal of Plant Physiology*, **22**, 987–1000.
- Loveland TR, Merchant JW, Ohlen DO *et al.* (1991) Development of a cover characteristics database for the conterminous US. *Photogrammetric Engineering and Remote Sensing*, **57**, 1453–1463.
- Major DJ, Beasley BW, Hamilton RI (1991) Effect of maize maturity on radiation-use efficiency. *Agronomy Journal*, **83**, 895–903.
- Massman WJ (1992) A surface energy balance method for partitioning evapotranspiration data into plant and soil components for a surface with partial canopy cover. *Water Resources Research*, **28**, 1723–1732.
- Massman WJ, Lee X (2002) Eddy covariance flux corrections and uncertainties in long term studies of carbon and energy exchange. *Agricultural and Forest Meteorology*, **113**, 121–144.
- Mebrahtu T, Hanover JW, Layne DR *et al.* (1991) Leaf temperature effects on net photosynthesis, dark respiration, and photorespiration of seedlings of black locust families with contrasting growth rates. *Canadian Journal of Forest Research*, **21**, 1616–1621.
- Middleton EM, Sullivan JH, Bovard BD *et al.* (1997) Seasonal variability in foliar characteristics and physiology for boreal forest species at the five Saskatchewan tower sites during the 1994 Boreal Ecosystem-Atmosphere Study. *Journal of Geophysical Research*, **102**, 28831–28844.
- Morecroft MD, Roberts JM (1999) Photosynthesis and stomatal conductance of mature canopy Oak (*Quercus robur*) and Sycamore (*Acer pseudoplatanus*) trees throughout the growing season. *Functional Ecology*, **13**, 332–342.
- Norman JM, Campbell GS (1989) Canopy structure. In: *Plant Physiological Ecology: Field Methods and Instrumentation* (eds Pearcy RW, Mooney HA, Ehleringer JR *et al.*), pp. 301–325. Chapman & Hall, New York.
- Norman JM, Garcia R, Verma SG (1991) Soil surface CO<sub>2</sub> fluxes and the carbon budget of a grassland. *Journal of Geophysical Research*, **97**, 18845–18853.
- Nouvellon Y, Seen DL, Rambal S *et al.* (2000) Time course of radiation use efficiency in a shortgrass ecosystem: consequences for remotely sensed estimation of primary production. *Remote Sensing of Environment*, **71**, 43–55.
- Oechel WC, Vourlitis GL, Verfaillier J, Jr. *et al.* (2000) A scaling approach for quantifying the net CO<sub>2</sub> flux of the Kuparuk river basin, Alaska. *Global Change Biology*, **6**, 160–173.
- Pierce LL, Running SW, Walker J (1994) Regional-scale relationships of leaf area index to specific leaf area and leaf nitrogen content. *Ecological Applications*, **4**, 313–321.
- Polley HW, Norman JM, Arkebauer TJ *et al.* (1992) Leaf gas exchange of *Andropogon gerardii* Vitman, *Panicum virgatum* L. and *Sorghastrum nutans* (L.) Nash in a tallgrass prairie. *Journal of Geophysical Research*, **97**, 18837–18844.
- Rayment MB, Jarvis PG (1999) Seasonal gas exchange of black spruce using an automatic branch bag system. *Canadian Journal of Forest Research*, **29**, 1528–1538.
- Reich PB, Ellsworth DS, Walters MB *et al.* (1999a) Generality of leaf trait relationships: a test across six biomes. *Ecology*, **80**, 1955–1969.
- Reich PB, Turner DP, Bolstad P (1999b) An approach to spatially-distributed modeling of net primary production (NPP) at the landscape scale and its application in validation of EOS NPP products. *Remote Sensing of Environment*, **70**, 69–81.
- Rochette P, Desjardins RL, Pattey E *et al.* (1996) Instantaneous measurement of radiation and water use efficiencies of a maize crop. *Agronomy Journal*, **88**, 627–635.
- Ruimy A, Jarvis PG, Baldocchi DD *et al.* (1995) CO<sub>2</sub> fluxes over plant canopies and solar radiation: a review. *Advances in Ecological Research*, **26**, 1–53.
- Ruimy A, Kergoat L, Field CB *et al.* (1996) The use of CO<sub>2</sub> flux measurements in models of the global terrestrial carbon budget. *Global Change Biology*, **2**, 287–296.
- Running SW, Thornton PE, Nemani R *et al.* (2000) Global terrestrial gross and net primary productivity from the Earth observing system. In: *Methods in Ecosystem Science* (eds Sala

- OE, Jackson RB, Mooney HA *et al.*), pp. 44–57. Springer, New York.
- Ryan MG, Lavigne MB, Gower ST (1997) Annual carbon cost of autotrophic respiration in boreal forest ecosystems in relation to species and climate. *Journal of Geophysical Research*, **102**, 28871–28884.
- Saugier B, Roy J, Mooney HA (2001) Estimations of global terrestrial productivity: converging toward a single number? In: *Terrestrial Global Productivity* (eds Roy J, Saugier B, Mooney HA), pp. 543–557. Academic Press, San Diego.
- Schimel DS, Kittel TG, Knapp AK *et al.* (1991) Physiological interactions along resource gradients in a tallgrass prairie. *Ecology*, **72**, 672–684.
- Sinclair TR, Horie T (1989) Leaf nitrogen, photosynthesis, and crop radiation use efficiency: a review. *Crop Science*, **29**, 90–98.
- SURFRAD (2001) <http://www.srrb.noaa.gov/surfrad/surfrpage.htm>.
- Teskey RO, Gholz HL, Cropper WP, Jr. (1994) Influence of climate and fertilization on net photosynthesis of mature slash pine. *Tree Physiology*, **14**, 1215–1227.
- Teskey RO, Sheriff DW, Hollinger DY *et al.* (1995) External and internal factors regulating photosynthesis. In: *Resources Physiology of Conifers: Acquisition, Allocation, and Utilization* (eds Smith WK, Hinkley TM), pp. 105–142. Academic Press, San Diego.
- Thornton PE, Running SW (1999) An improved algorithm for estimating incident daily solar radiation from measurements of temperature, humidity, and precipitation. *Agricultural and Forest Meteorology*, **93**, 211–228.
- Tollenaar M, Bruulsema TW (1988) Efficiency of maize dry matter production during periods of complete leaf area expansion. *Agronomy Journal*, **80**, 580–585.
- Turner DP, Gower ST, Cohen WB *et al.* (2002) Effects of spatial variability in light use efficiency on satellite-based NPP monitoring. *Remote Sensing of Environment*, **80**, 397–405.
- Villar R, Held AA, Merino J (1995) Dark leaf respiration in light and darkness of an evergreen and a deciduous plant species. *Plant Physiology*, **107**, 421–427.
- White MA, Thornton PE, Running SW (1997) A continental phenology model for monitoring vegetation responses to interannual climatic variability. *Global Biogeochemical Cycles*, **11**, 217–234.
- Williams M, Malhi Y, Nobre D *et al.* (1998) Seasonal variation in net carbon exchange and evapotranspiration in a Brazilian rain forest: a modeling analysis. *Plant, Cell and Environment*, **21**, 953–968.
- Williams M, Rastetter EB, Shaver GR *et al.* (2001) Primary production in an arctic watershed: an uncertainty analysis. *Ecological Applications*, **11**, 1800–1816.
- Wofsy SC, Goulden ML, Munger JW *et al.* (1993) Net exchange of CO<sub>2</sub> in a mid-latitude forest. *Science*, **260**, 1314–1317.
- Woodward FI, Smith TM (1994) Predictions and measurements of the maximum photosynthetic rate,  $A_{max}$ , at the global scale. In: *Ecophysiology of Photosynthesis* (eds Schultze E-D, Caldwell MM), pp. 491–509. Springer, Berlin.